_____

Original Communication

SPATIAL AND STRUCTURAL COMPLEXITY OF CEREBRAL HEMISPHERES IN MALE AND FEMALE BRAIN: FRACTAL AND QUANTITATIVE ANALYSES OF MRI BRAIN SCANS

Nataliia Maryenko, Oleksandr Stepanenko

Department of Histology, Cytology and Embryology, Kharkiv National Medical University, Kharkiv, Ukraine

ABSTRACT

Objectives: The aim of the present study was to compare the features of the structural complexity of the cerebral hemispheres in men and women using fractal analysis of outlined and skeletonized images, as well as quantitative analysis of digital skeletons of the cerebral hemispheres. Material and Methods: Magnetic resonance imaging brain scans of 100 individuals aged 18-86 years (44 males and 56 females) were investigated. Five sections of each brain were selected for morphometric study (4 coronal and 1 axial sections). The sections were preprocessed, and outlined and skeletonized images were obtained. Fractal analysis was conducted using the two-dimensional box counting method, and fractal dimensions of outlined and skeletonized images were determined. Additionally, quantitative analysis of skeletonized images was performed, determining the following parameters: branches, junctions, end-point voxels, junction voxels, slab voxels, triple points, quadruple points, average branch length, and maximum branch length. Results: We observed that both variants of fractal dimension in males and females did not show significant differences, although most quantitative parameters in males were larger than those in females. Conclusions: The spatial and structural complexity of the cerebral hemispheres, as characterized by fractal dimensions, is almost indistinguishable between males and females. However, in some individual brain sections, the male brain may exhibit a slightly higher number of end-point voxels, corresponding to the gyri of the cerebral hemispheres. The obtained data can be used in clinical practice for diagnostic purposes (e.g., for detecting malformations) and for theoretical studies in neuroanatomy.

Key words: cerebrum, fractal dimension, gender, neuroimaging

RESUMEN

Objetivos: El objetivo del presente estudio fue comparar las características de la complejidad estructural de los hemisferios cerebrales en hombres y mujeres mediante el análisis fractal de imágenes delineadas y esqueletizadas, así como el análisis cuantitativo de esqueletos digitales de los hemisferios cerebrales. Material y Métodos: Se investigaron resonancias magnéticas cerebrales de 100 individuos de 18 a 86 años (44 hombres y 56 mujeres). Se seleccionaron cinco secciones de cada cerebro para el estudio morfométrico (4 secciones coronales y 1 axial). Las secciones fueron preprocesadas y se obtuvieron imágenes delineadas y esqueletizadas. Se realizó un análisis fractal utilizando el método de conteo de cajas bidimensional, y se determinaron las dimensiones fractales de las imágenes delineadas y esqueletiza- das. Además, se llevó a cabo un análisis cuantitativo de las imágenes esqueletizadas, determinando los siguientes parámetros: ramas, intersecciones, voxels de punto final, voxels de intersección, voxels de losas, puntos triples, puntos cuádruples, longitud promedio de la rama y longitud máxima de la rama. Resultados: Observamos que ambas variantes de dimensión fractal en hombres y mujeres no mostraron diferencias significativas, aunque la mayoría de los parámetros cuantitativos en hombres fueron mayores que en mujeres. Conclusiones: La complejidad espacial y estructural de los hemisferios cerebrales, caracterizada por dimensiones fractales, es casi indistinguible entre hombres y mujeres. Sin embargo, en algunas secciones individuales, el cerebro masculino puede mostrar un número ligeramente mayor de voxels de punto final, correspondientes a los giros de los hemisferios cerebrales. Los datos obtenidos se pueden utilizar en la práctica clínica con fines diagnósticos (por ejemplo, para detectar malformaciones) y para estudios teóricos en neuroanatomía.

Palabras clave: cerebro, dimensión fractal, género, neuroimagen

_____

* *Correspondence to*: **Nataliia Maryenko.** ni.marienko@knmu.edu.ua

_____

INTRODUCTION

The brain structures, including the cerebral hemispheres, exhibit a complex shape, determined by their spatial and structural complexity. Spatial complexity characterizes the intricacy, irregularity of shape, its convolutions, or branching, and structural complexity describes the features of the composition of a specific structure: how many component elements constitute it, and how intricate their configuration and combinations are. The spatial and structural complexity of the cerebral hemispheres is primarily manifested in the number of gyri and sulci, the complexity of their configuration – characteristics influencing the overall shape complexity of the cerebral hemispheres (Hofman, 1991; Kiselev et al., 2003). Quantitative assessment of these parameters is valuable for diagnosing brain malformations, characterizing brain development in ontogenesis, and detecting and quantitatively characterizing age-related changes in the brain (Kalmanti and Maris, 2007; De Luca et al., 2016; Farahibozorg et al., 2015; Podgórski et al., 2021).

The differences in the structural organization of the male and female brains are of great interest, being crucial for interpreting brain research data for diagnostic purposes and for theoretical neuroanatomical studies (Savic and Arver, 2011; Farahibozorg et al., 2015; Király et al., 2016; Brennan et al., 2021; Podgórski et al., 2021). It is known that the male brain exhibits larger dimensions and volume compared to the female brain (Király et al., 2016). However, open questions persist: Does the spatial and structural complexity of the brain differ between men and women? Do differences in brain size lead to changes in its spatial configuration? Answers to these questions can be obtained through a comparative analysis of morphometric data. However, the spatial configuration of the cerebral hemispheres cannot be comprehensively characterized as the shape of a simple geometric figure, complicating the morphometric assessment of brain structures using classical morphometry methods (measurement of linear dimensions, area, volume) based on Euclidean geometry.

In recent decades, fractal analysis, a method derived from fractal geometry (Mandelbrot, 1982), is increasingly employed in medicine and morphology. The parameter determined through fractal analysis is the fractal dimension, a measure of the spatial filling capacity of the investigated structure. With the increase in the spatial and structural complexity of certain formations, the degree of space filling also increases, leading to an increase in the values of the fractal dimension. Therefore, the fractal dimension of brain structures allows for a quantitative assessment of their spatial and structural complexity (Lee et al., 2004; Ha et al., 2005; Im et al., 2006; Zhang et al., 2006, 2007, 2008; Kalmanti and Maris, 2007; King et al., 2009; Goñi et al., 2013; Di Ieva et al., 2015; Farahibozorg et al., 2015; Madan and Kensinger, 2016; Podgórski et al., 2021).

The fractal dimension can be determined both for the entire structure and its individual components. Various preprocessing techniques can be applied for fractal analysis, such as contour tracing, or outlining (resulting in outlined images) and skeletonizing (resulting in skeletonized images, representing the digital skeleton of a particular structure) (Jelinek and Fernandez, 1998; Milosević and Ristanović, 2006). In previous studies, various researchers have investigated the cortical ribbon (Hofman, 1991; Kiselev et al., 2003; King et al., 2009; Goñi et al., 2013; Madan and Kensinger, 2016; Podgórski et al., 2021), the outer (pial) surface of the cortex or its contours (Lee et al., 2004; Ha et al., 2005; Im et al., 2006; Kalmanti and Maris, 2007; Goñi et al., 2013; Madan and Kensinger, 2016), the white matter as a whole (Goñi et al., 2013; Farahibozorg et al., 2015), and digital skeletons of white matter (Zhang et al., 2006, 2007, 2008; Farahibozorg et al., 2015).

In addition to the fractal analysis, a quantitative analysis of skeletonized images can be performed. This method of image analysis is primarily used in studies of neurons and their dendritic trees (Li et al., 2019; Jiang et al., 2020). In our previous works, we conducted a fractal analysis of the contour (Maryenko and Stepanenko, 2023) and digital skeletons of the cerebral hemispheres (Maryenko and Stepanenko, 2022a) and, for the first time, attempted to perform quantitative analysis of skeletonized images of the cerebral hemispheres (Maryenko and Stepanenko, 2022b). In this study, our aim was to compare the features of the structural complexity of the cerebral hemispheres in men and women using fractal analysis of outlined and skeletonized images, as well as quantitative analysis of digital skeletons of the cerebral hemispheres.

MATERIAL AND METHODS

In this study, we examined magnetic resonance imaging (MRI) brain scans of 100 individuals aged 18-86 years (average age 41.72±1.58

_____

years). The study sample included 44 males (average age 41.43±1.68 years, minimum – 18 years, maximum – 86 years) and 56 females (average age 41.95±1.51 years, minimum – 18 years, maximum – 72 years). The individuals included in the study sample underwent MRI

brain scanning for diagnostic purposes, and no morphological changes in the structures of the brain and surrounding areas were detected. These individuals were considered to be conditionally healthy, and the structure of the brain was deemed to be within normal conditions.
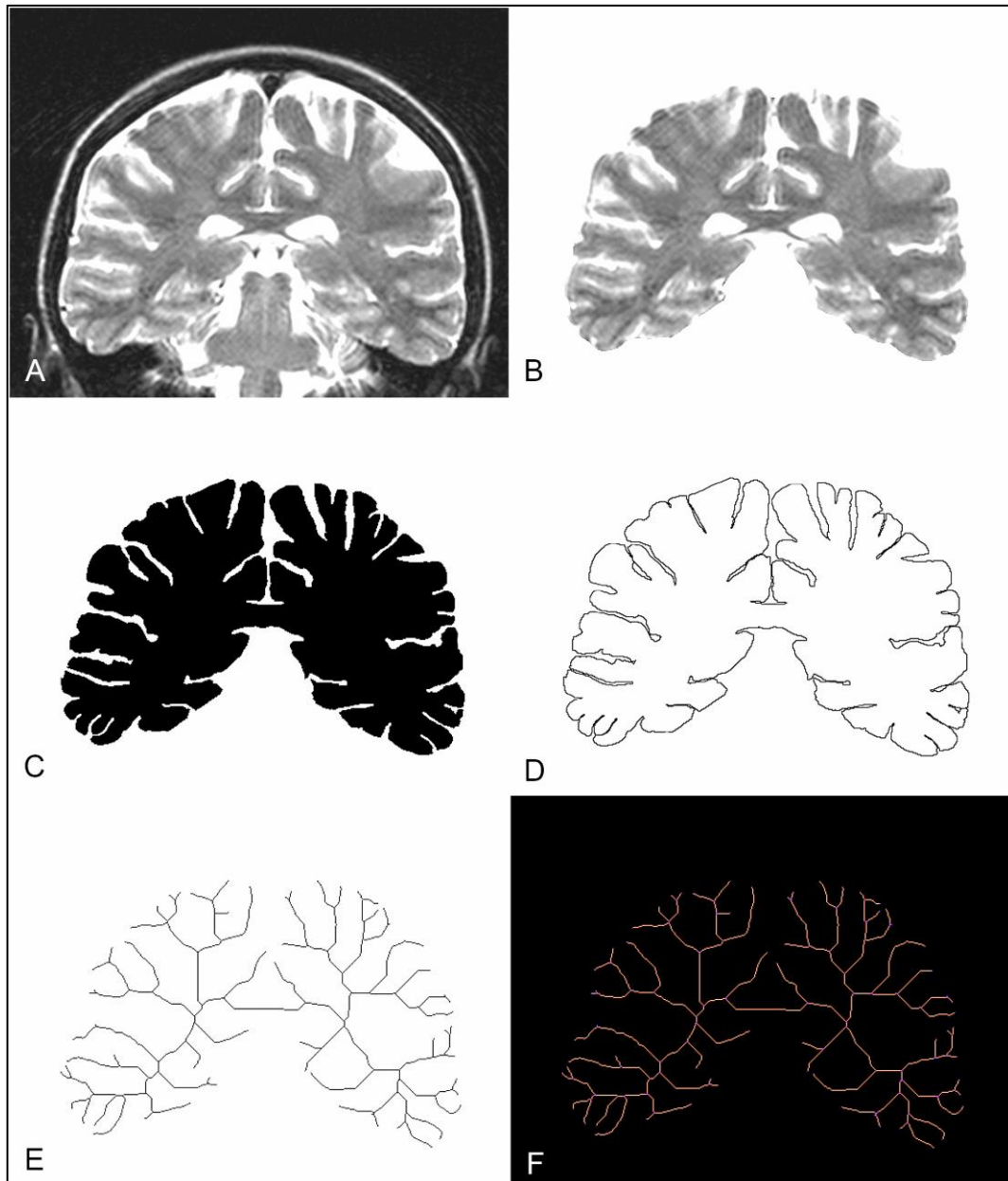
Figure 1- Preprocessing and quantitative analysis of MRI brain images: A – MRI brain scan (3rd coronal section); B – background removal; C – segmentation resulting in the silhouette brain image; D – contour outlining resulting in the outlined brain image; E – image skeletonizing resulting in the skeletonized image; F – quantitative analysis of the digital skeleton

Brain scans were obtained using the MRI scanner Siemens Magnetom Symphony with a magnetic induction value of 1.5 Tesla. T2 and

FLAIR sequences were employed. The MRI parameters were as follows: T2 sequence: TE (echo time) – 130 ms, TR (repetition time) – 4440

_____

ms; FLAIR sequence: TE (echo time) – 114 ms, TR (repetition time) – 9000 ms, TI (inversion time) – 2500 ms. The section thickness for both sequences was 5 mm. The digital MRI image resolution was 72 pixels per inch, and the absolute image scale was 3 pixels = 1 mm.

From the set of MRI images of each brain, 5 brain sections were selected, including 4 sections in the coronal projection and 1 in the axial projection. The first coronal section was positioned at the level of the most anterior points of the temporal lobes, the 2nd at the level of the mammillary bodies, the 3rd at the level of the quadrigeminal plate, the 4th at the level of the splenium of the corpus callosum, and the axial brain section was positioned at the level of the thalamus. These sections were selected based on the following criteria: localization in different regions of the cerebral hemispheres, easy identification using anatomical landmarks, and correspondence to areas where pathological changes are most frequently detected in neurodegenerative diseases (e.g., Alzheimer's disease) (King et al., 2009).

After selecting the images, they underwent preprocessing (Fig. 1). Images with a resolution of 128 pixels per inch and the following dimensions were created using Adobe Photoshop CS5: for the study of coronal sections – 512×400 pixels, for axial sections – 512×800 pixels. A fragment of the digital MRI image corresponding to the area under investigation was inserted into a previously created image. In this process, the fragment was positioned to ensure that the section of the cerebral hemispheres was fully accommodated within the created image and did not extend beyond its borders (Fig. 1, A).

In the subsequent preprocessing phase, background structures were eliminated from the image, as illustrated in Figure 1, B. Following this step, an initial or "rough" segmentation process was implemented through thresholding. This involved applying a predetermined threshold brightness value for pixels: pixels with brightness values below the specified threshold were assigned a black color, while those surpassing the threshold were rendered in white. In the case of images acquired using the T2 sequence, a median brightness threshold value of 128 was utilized; for images obtained through the FLAIR sequence, a threshold value of 65 was utilized.

Subsequently, a manual correction process was applied for achieving a "precise" segmentation, aiming to enhance the anatomical accuracy of the acquired images. This correction involved the use of tools within the Adobe Photoshop CS5 software. Consequently, the segmentation of MRI images resulted in the generation of binary silhouette representations of the cerebral hemispheres, as depicted in Figure 1, C.

For further image processing and analysis stages, the Image J software (Schneider et al., 2012) was utilized. From the binary silhouette images, outlined and skeletonized images were obtained. Silhouette images were outlined using the "outline" tool (Fig. 1, D), with a contour line thickness of 1 pixel. Skeletonizing of silhouette images was carried out using the "skeletonize" tool (Fig. 1, E). This tool transforms the silhouette image into its digital skeleton by eroding the silhouette into lines with a thickness of 1 pixel.

After the preprocessing, a fractal analysis of outlined and skeletonized images was conducted using the box counting method, employing the "fractal box count" tool of the Image J software. The fractal dimension values were determined for outlined images (fractal dimension of the contour, FDo) and skeletonized images (fractal dimension of the digital skeleton, FDs). FDo and FDs values were determined for each of the five brain sections, and their arithmetic mean values were calculated.

The next stage of the study, aimed at complementing the fractal analysis, involved a quantitative analysis of digital skeletons. For this stage, the "analyze skeleton" tool of the Image J software was utilized (Fig. 1, E). In each of the digital skeletons, the following parameters were determined: branches, junctions, end-point voxels, junction voxels, slab voxels, triple points, quadruple points, average branch length, maximum branch length. The "branches" parameter characterizes the number of branches of digital skeleton, while "junctions" represents the number of branch connections. The "end-point voxels" parameter corresponds to the number of end points of the digital skeleton branches, "junction voxels" is the number of voxels (pixels) forming branch junctions, and "slab voxels" is the number of voxels forming branches. The "triple points" parameter indicates the number of junctions connecting three branches, and "quadruple points" represent junctions connecting four branches. The "average branch length" is the arithmetic mean of the absolute length of all branches, and the "maximum branch length" is the maximum value among the absolute lengths of all branches of the digital skeleton.

Statistical data processing was carried out using Microsoft Excel 2016. For each dataset, the mean (M) and standard deviation (σ) were calculated. The significance of statistical differences between fractal dimension values and parameters of digital skeletons in males and females was determined using the Student's T-test. To assess the relationships between the

_____

obtained values, the Pearson correlation coefficient (r) was calculated. The significance level for all results was accepted as $P < 0.05$.

Parameter	Sex group	Value	Brain section					
			1st coronal	2nd coronal	3rd coronal	4th coronal	axial	Average value (all sections)
Fractal dimension (outlined images)	Male	M	1.287	1.253	1.247	1.245	1.232	1.253
		σ	0.028	0.027	0.023	0.017	0.027	0.015
	Female	M	1.285	1.250	1.240	1.240	1.234	1.250
		σ	0.023	0.032	0.024	0.021	0.030	0.016
		P	0.352	0.319	0.072	0.122	0.380	0.182
Fractal dimension (skeletonized images)	Male	M	1.206	1.163	1.154	1.156	1.141	1.164
		σ	0.029	0.027	0.026	0.026	0.024	0.017
	Female	M	1.208	1.161	1.158	1.160	1.136	1.165
		σ	0.026	0.035	0.031	0.026	0.023	0.019
		P	0.319	0.378	0.221	0.233	0.164	0.407
Branches, N	Male	M	96.8	131.5	123.1	116.2	159.4	125.8
		σ	16.2	26.7	25.1	20.0	49.9	18.7
	Female	M	94.1	120.0	118.6	116.7	143.2	118.5
		σ	15.5	26.8	25.4	23.8	38.2	16.4
		P	0.198	*0.018*	0.187	0.462	*0.038*	*0.023*
Junctions, N	Male	M	49.4	67.6	63.2	59.5	82.1	64.6
		σ	9.4	15.6	14.6	11.6	27.1	10.8
	Female	M	48.0	61.1	61.1	60.0	73.4	60.7
		σ	9.0	14.8	14.9	13.3	20.9	9.2
		P	0.223	*0.017*	0.241	0.429	*0.040*	*0.031*
End-point voxels, N	Male	M	42.6	56.6	53.9	50.9	68.4	54.5
		σ	5.2	7.6	6.6	5.9	17.1	5.5
	Female	M	41.2	53.3	51.1	50.2	63.5	51.8
		σ	5.6	9.0	7.2	8.0	12.7	5.3
		P	0.100	*0.027*	*0.025*	0.317	*0.056*	*0.009*
Junction voxels, N	Male	M	158.4	212.6	196.2	184.8	248.2	200.7
		σ	33.6	55.5	50.7	38.0	92.6	35.9
	Female	M	154.8	188.8	191.3	187.0	224.1	189.5
		σ	32.8	52.1	52.0	46.2	74.9	31.4
		P	0.296	*0.015*	0.320	0.396	0.082	*0.055*
Slab voxels, N	Male	M	1797.6	2747.6	2745.1	2728.1	4421.5	2895.6
		σ	194.1	310.9	276.2	259.5	679.5	247.3
	Female	M	1721.5	2583.0	2628.1	2590.5	4047.1	2717.6
		σ	201.3	318.8	266.8	237.5	481.3	211.9
		P	*0.030*	*0.006*	*0.017*	*0.003*	*0.001*	*<0.001*
Triple points, N	Male	M	46.3	63.8	60.1	56.5	77.8	61.1
		σ	8.1	13.8	13.2	10.9	24.7	9.8
	Female	M	44.9	57.5	58.1	56.6	70.1	57.4
		σ	8.0	12.8	13.5	12.2	18.7	8.2
		P	0.187	*0.010*	0.223	0.475	*0.042*	*0.025*
Quadruple points, N	Male	M	2.3	3.0	2.5	2.3	3.8	2.8
		σ	1.7	2.3	1.8	1.6	3.6	1.1
	Female	M	2.3	3.1	2.4	2.6	2.7	2.6
		σ	1.7	2.7	1.8	1.8	2.6	1.1
		P	0.417	0.480	0.302	0.272	*0.045*	0.127
Average branch length, mm	Male	M	8.48	9.24	9.77	10.28	12.42	10.04
		σ	1.03	0.99	1.01	0.99	1.65	0.65
	Female	M	8.24	9.47	9.74	9.83	12.56	9.98
		σ	0.88	0.89	1.07	1.06	1.69	0.64
		P	0.106	0.109	0.454	*0.016*	0.338	0.317
Maximum branch length	Male	M	27.72	34.32	36.91	40.23	50.15	37.87
		σ	4.48	6.35	6.25	6.73	8.94	3.20
	Female	M	26.89	33.58	37.86	40.42	51.44	38.10
		σ	5.48	4.78	6.06	5.81	9.24	3.06
		P	0.211	0.254	0.221	0.440	0.247	0.362

_____

Table 1- Descriptive statistics of the fractal dimension values and quantitative parameters of digital skeletons of the cerebral hemispheres in male and female brain. Note: P values were obtained by Student T test assessing difference between parameters in male and female groups

RESULTS

The values of fractal dimension and parameters of the digital skeletons of the cerebral hemispheres in males and females are presented in Table 1. The values of FDo and FDs in males and females were similar and did not differ significantly (P>0.05 for all investigated images). However, the FDo values for most brain sections were slightly higher in males, while the FDs values were slightly higher in females.

In comparing the parameters of the digital skeletons of the cerebral hemispheres, it was found that most parameters were higher in males than in females. However, the difference was significant not for all parameters and not for all sections. Specifically, the number of branches and their junctions was higher in males than in females, and the difference was significant for the 2nd coronal and axial sections and the average value of the five sections. The number of end-point voxels in the digital skeletons was also higher in males for most sections, with a significant difference for the 2nd, 3rd coronal sections, and the average value of the five sections. The number of junction voxels was slightly higher in males for most sections (except the 4th coronal section), with a significant difference only for the 2nd coronal section. The most significant differences were observed in the number of slab voxels: this parameter was significantly higher in males in all investigated brain sections. The number of triple points was higher in males in most locations (except the 4th coronal section), with a significant difference for the 2nd coronal and axial sections and the average value of the five sections. However, differences in the number of quadruple points varied: in some sections, this parameter was higher in males (3rd coronal and axial sections), while in others, it was higher in females (2nd and 4th coronal sections), with a significant difference only for the axial section. These characteristics indicate the heterogeneity of this parameter both overall and in different brain sections. The average branch length was greater in males for most sections (except the 2nd coronal and axial sections), with a significant difference only for the 4th coronal section. The maximum branch length did not differ significantly between males and females.
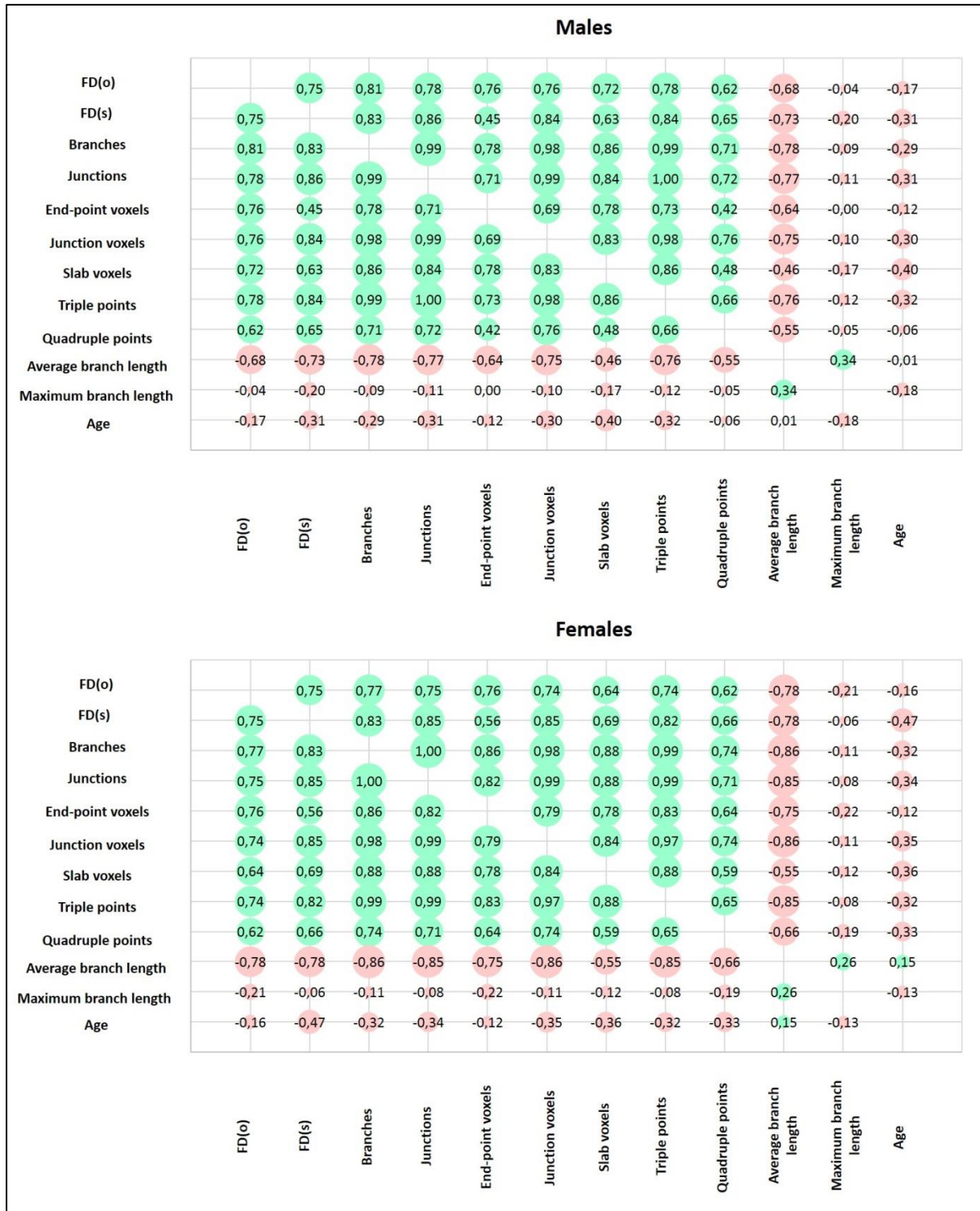
During the correlation analysis (Graphic 1), it was observed that the correlation relationships between the studied parameters in males and females were highly similar. It was determined that FDo and FDs, along with the majority of investigated quantitative parameters of digital skeletons (branches, junctions, end-point voxels, junction voxels, slab voxels, triple points, quadruple points), exhibited strong and moderate positive correlations with each other (P < 0.05). In contrast, the average and maximum branch length showed negative correlations with the remaining parameters and positive correlations with each other. Based on this, all studied parameters can be categorized into two groups: the first group includes FDo and FDs and quantitative parameters of digital skeletons, excluding average and maximum branch length, which belong to the second group.

As the values of the first group increase, the values of the other parameters within this group also increase. When the silhouette of the cerebral hemispheres becomes more complex on a specific brain section, it results in an increase in both fractal dimension values – FDo and FDs. Since an increase in the number of gyri corresponds to an increase in the spatial complexity of the configuration of the cerebral hemispheres' surface, it leads to an increase in the values of the fractal dimension of the outlined images (FDo). The increase in the number of gyri also leads to an increase in the number of end-point voxels in the digital skeleton. The increase in the complexity of the spatial configuration also leads to an increase in the complexity of the digital skeleton, resulting in both an increase in the number of branches and their junctions and an increase in the values of the fractal dimension of the skeletonized images (FDs). Notably, the number of end-point voxels has stronger correlation relationships with the fractal dimension of the contour (FDo), reflecting the complexity of the configuration of the outer surface of the cerebral hemispheres primarily determined by the number of gyri, than with the fractal dimension of the digital skeletons (FDs), which is more associated with the "internal complexity" of the digital skeleton, determined by the number of inner branches and their junctions.

The second group of studied parameters includes the average and maximum branch length, which decrease with an increase in the parameters of the first group and vice versa. Therefore, it can be concluded that the digital skeleton of the cerebral hemispheres with lower spatial and structural complexity consists of a small number of long branches, while the digital skeleton with greater complexity is characterized by a large number of short branches (i.e., the branches are "broken") and forms a more complex internal structure.

Additionally, we have found that the correlation relationships with age in males and females were close, and in most sections, they were almost indistinguishable. It was also established that the values of FDo almost did not change with age, as well as the values of end-point voxels, average, and maximum branch length. A moderate decrease in the values of FDs and the associated with it parameters of skeletonized images, such as branches, junctions, junction voxels, slab voxels, and triple points, was also identified.

Males

	FD(o)	FD(s)	Branches	Junctions	End-point voxels	Junction voxels	Slab voxels	Triple points	Quadruple points	Average branch length	Maximum branch length	Age
FD(o)		0,75	0,81	0,78	0,76	0,76	0,72	0,78	0,62	-0,68	-0,04	-0,17
FD(s)	0,75		0,83	0,86	0,45	0,84	0,63	0,84	0,65	-0,73	-0,20	-0,31
Branches	0,81	0,83		0,99	0,78	0,98	0,86	0,99	0,71	-0,78	-0,09	-0,29
Junctions	0,78	0,86	0,99		0,71	0,99	0,84	1,00	0,72	-0,77	-0,11	-0,31
End-point voxels	0,76	0,45	0,78	0,71		0,69	0,78	0,73	0,42	-0,64	-0,00	-0,12
Junction voxels	0,76	0,84	0,98	0,99	0,69		0,83	0,98	0,76	-0,75	-0,10	-0,30
Slab voxels	0,72	0,63	0,86	0,84	0,78	0,83		0,86	0,48	-0,46	-0,17	-0,40
Triple points	0,78	0,84	0,99	1,00	0,73	0,98	0,86		0,66	-0,76	-0,12	-0,32
Quadruple points	0,62	0,65	0,71	0,72	0,42	0,76	0,48	0,66		-0,55	-0,05	-0,06
Average branch length	-0,68	-0,73	-0,78	-0,77	-0,64	-0,75	-0,46	-0,76	-0,55		0,34	-0,01
Maximum branch length	-0,04	-0,20	-0,09	-0,11	0,00	-0,10	-0,17	-0,12	-0,05	0,34		-0,18
Age	-0,17	-0,31	-0,29	-0,31	-0,12	-0,30	-0,40	-0,32	-0,06	0,01	-0,18	

Females

	FD(o)	FD(s)	Branches	Junctions	End-point voxels	Junction voxels	Slab voxels	Triple points	Quadruple points	Average branch length	Maximum branch length	Age
FD(o)		0,75	0,77	0,75	0,76	0,74	0,64	0,74	0,62	-0,78	-0,21	-0,16
FD(s)	0,75		0,83	0,85	0,56	0,85	0,69	0,82	0,66	-0,78	-0,06	-0,47
Branches	0,77	0,83		1,00	0,86	0,98	0,88	0,99	0,74	-0,86	-0,11	-0,32
Junctions	0,75	0,85	1,00		0,82	0,99	0,88	0,99	0,71	-0,85	-0,08	-0,34
End-point voxels	0,76	0,56	0,86	0,82		0,79	0,78	0,83	0,64	-0,75	-0,22	-0,12
Junction voxels	0,74	0,85	0,98	0,99	0,79		0,84	0,97	0,74	-0,86	-0,11	-0,35
Slab voxels	0,64	0,69	0,88	0,88	0,78	0,84		0,88	0,59	-0,55	-0,12	-0,36
Triple points	0,74	0,82	0,99	0,99	0,83	0,97	0,88		0,65	-0,85	-0,08	-0,32
Quadruple points	0,62	0,66	0,74	0,71	0,64	0,74	0,59	0,65		-0,66	-0,19	-0,33
Average branch length	-0,78	-0,78	-0,86	-0,85	-0,75	-0,86	-0,55	-0,85	-0,66		0,26	0,15
Maximum branch length	-0,21	-0,06	-0,11	-0,08	-0,22	-0,11	-0,12	-0,08	-0,19	0,26		-0,13
Age	-0,16	-0,47	-0,32	-0,34	-0,12	-0,35	-0,36	-0,32	-0,33	0,15	-0,13	

_____

Graphic 1- Correlation relationships between fractal dimension values, quantitative parameters of digital skeletons of the cerebral hemispheres and age in male and female brain; graphic shows the values of Pearson's correlation coefficients (r)

DISCUSSION

In this study, our goal was to characterize and compare the spatial and structural complexity of the cerebral hemispheres in the male and female brain using the fractal dimensions of outlined and skeletonized images, along with quantitative parameters of digital skeletons. It was observed that both variants of fractal dimension in males and females did not show significant differences, although most quantitative parameters in males were larger than those in females.

The fractal dimension is a parameter of fractal geometry, and its values are independent of the scale and size of the structure. This parameter characterizes how a specific structure fills the available space. For example, the fractal dimension of the contour of cerebral hemispheres allows for a quantitative characterization of the complexity of the spatial configuration of the brain surface: the more gyri the hemispheres have, the more complex the configuration of their contour, and the more space the contour occupies. The number of end-point voxels, a parameter of skeletonized images corresponding to the number of endpoints formed by gyri, was closely associated with this indicator. Since the number of gyri remains constant throughout adulthood, a slight decrease in these parameters in some brain sections can be explained by a simplification of the gyrus shape observed in aging brains. The majority of brain sections showed no significant difference in these parameters between males and females. However, in the 2nd and 3rd coronal sections, the number of end-point voxels (and thus the number of gyri) in males was statistically significantly higher than in females, reflecting a moderate increase in FDo in men in the respective sections (although the difference from women was not significant). Therefore, it can be concluded that the male brain may be characterized by a slightly higher number of gyri in certain brain sections, but the overall spatial complexity of the surface, assessed using fractal dimension, is almost indistinguishable between males and females.

The fractal dimension of the digital skeleton in males and females also did not differ significantly. However, this value of fractal dimension was associated with parameters of the digital skeleton, which were larger in males than in females and decreased with age: these included branches, junctions, junction voxels, slab voxels, and triple points. In our previous study (Maryenko and Stepanenko, 2022b), it was

found that the mentioned quantitative parameters of digital skeletons had positive correlation relationships with the area of brain sections. Thus, a decrease in the silhouette area during skeletonizing will lead to the formation of a skeleton with fewer internal branches and their connections, resulting in a decrease in fractal dimension values. Therefore, gender differences in the values of the studied quantitative parameters can be explained by the difference in the sizes of the male and female brains. The age-related decrease in the values of quantitative parameters of digital skeletons reflects not the structural complexity of the brain but rather the overall reduction in the size of the brain.

Previous works by other researchers were primarily focused on values of fractal dimension, but a quantitative analysis of skeletonized images by other authors has not been conducted. Among the studies related to fractal analysis, several compared the values of fractal dimension in males and females, including the fractal dimension of the cerebral cortex (Podgórski et al., 2021), the outer surface of the cortex (Lee et al., 2004), white matter as a whole (Farahibozorg et al., 2015), and the digital skeletons of white matter (Zhang et al., 2007; Farahibozorg et al., 2015).

In the work of Lee et al. (2004), a fractal analysis of skeletonized images of the brain surface was conducted (N=62, 34 males and 28 females). The authors found that the values of fractal dimension in males and females did not significantly differ, while the volumes of gray and white matter in males were significantly higher. This study is similar to ours, but the authors conducted a fractal analysis of the skeletonized surface, whereas in our study, the outlined contour was studied.

In the study by Zhang et al. (2007), a fractal analysis of the digital skeletons of cerebral white matter was conducted (N=36, 17 males and 19 females). It was found that the fractal dimension in males was higher than in females, suggesting a greater complexity of the brain structure in males. In our study, the fractal dimension of digital skeletons was also determined, but not of white matter, but of the cerebral hemispheres as a whole. In our study, the fractal dimension of digital skeletons in males and females did not differ.

In the study by Farahibozorg et al. (2015), the aging characteristics of the brain in men and women were investigated (N=209, 95 males and 114 females). The study examined the values of fractal dimension of white matter: its volume,

_____

surface, and digital skeletons. It was found that the fractal dimension of the surface in males and females did not differ, but the fractal dimension of the volume and digital skeletons of white matter in males was higher than in females. The authors identified that the values of fractal dimension in males and females decreased with age, and after normalizing the data for brain volume, the age-related dynamics in men and women were similar.

In the study by Podgórski et al. (2021), the focus was on determining the age dynamics of morphometric indicators in men and women, including fractal dimension (N=697, 264 males and 443 females). The results showed that cortical fractal dimensions changed during aging only in a small percentage of locations in males (2.0%), while in females, this percentage was significantly higher (2.7%). The authors stated that male and female brains begin aging at a similar age of 45, but compared to men, in women, the cortex is affected earlier and in a more complex pattern.

Therefore, the fractal dimensions of outlined and skeletonized images and quantitative parameters of digital skeletons of the cerebral hemispheres allow for a quantitative characterization of the spatial and structural complexity of the brain. The fractal dimension of contours and the number of end-point voxels are less sensitive to age-related changes and primarily characterize innate characteristics, while other parameters of skeletonized images depend more on the size of the brain, resulting in significant differences in these characteristics between males and females and a decrease in these parameters with age. In our opinion, for diagnostic purposes (e.g., for detecting malformations), it is advisable to use a comprehensive combination of these parameters. Despite the fact that the male brain is characterized by larger sizes, the spatial and structural complexity of the cerebral hemispheres, characterized by fractal dimensions (which are independent of size), is almost indistinguishable between males and females. However, in some individual brain sections, male brain may exhibit a slightly higher number of end-point voxels, corresponding to the gyri of the cerebral hemispheres.

Conflict of interest
None.

Ethical approval
The study was conducted in accordance with the Declaration of Helsinki, and approved by the Commission on Ethics and Bioethics of Kharkiv National Medical University (minutes of the meeting of the Commission on Ethics and Bioethics of KhNMU No. 10 of Nov. 7, 2018) for studies involving humans.

Informed consent
Written informed consent has been obtained from the participants of the study.

Contributions
N.M.: Conceptualization; Data curation; Formal analysis; Investigation; Methodology; Software; Visualization; Writing – original draft. O.S.: Conceptualization; Project administration; Supervision; Validation; Writing – review & editing.

ACKNOWLEDGMENTS

REFERENCES

Brennan D, Wu T, Fan J. 2021. Morphometrical brain markers of sex difference. Cerebral Cortex 31: 3641–49.

De Luca A, Arrigoni F, Romaniello R, Triulzi FM, Peruzzo D, Bertoldo A. 2016. Automatic localization of cerebral cortical malformations using fractal analysis. Physics in Medicine and Biology 61: 6025–40.

Di Ieva A, Esteban FJ, Grizzi F, Klonowski W, Martín-Landrove M. 2015. Fractals in the neurosciences, Part II: Clinical applications and future perspectives. The Neuroscientist 21: 30-43.

Farahibozorg S, Hashemi-Golpayegani SM, Ashburner J. 2015. Age- and sex-related variations in the brain white matter fractal dimension throughout adulthood: an MRI study. Clinical Neuroradiology 25: 19–32.

_____

Goñi J, Sporns O, Cheng H, Aznárez-Sanado M, Wang Y, Josa S, Arrondo G, Mathews VP, Hummer TA, Kronenberger WG, Avena-Koenigsberger A, Saykin AJ, Pastor MA. 2013. Robust estimation of fractal measures for characterizing the structural complexity of the human brain: optimization and reproducibility. NeuroImage 83: 646-57.

Ha TH, Yoon U, Lee KJ, Shin YW, Lee JM, Kim IY, Ha KS, Kim SI, Kwon JS. 2005. Fractal dimension of cerebral cortical surface in schizophrenia and obsessive-compulsive disorder. Neuroscience Letters 384: 172-76.

Hofman MA. 1991. The fractal geometry of convoluted brains. Journal of Hirnforschung.32: 103-11.

Im K, Lee JM, Yoon U, Shin YW, Hong SB, Kim IY, Kwon JS, Kim SI. 2006. Fractal dimension in human cortical surface: multiple regression analysis with cortical thickness, sulcal depth, and folding area. Human Brain Mapping 27: 994-1003.

Jelinek HF, Fernandez E. 1998. Neurons and fractals: how reliable and useful are calculations of fractal dimensions? Journal of Neuroscience Methods 81: 9-18.

Jiang S, Pan Z, Feng Z, Guan Y, Ren M, Ding Z, Chen S, Gong H, Luo Q, Li A. 2020. Skeleton optimization of neuronal morphology based on three-dimensional shape restrictions. BMC Bioinformatics 21: 395.

Kalmanti E, Maris TG. 2007. Fractal dimension as an index of brain cortical changes throughout life. In vivo 21: 641–46.

King RD, George AT, Jeon T, Hynan LS, Youn TS, Kennedy DN, Dickerson B; Alzheimer's Disease Neuroimaging Initiative. 2009. Characterization of atrophic changes in the cerebral cortex using fractal dimensional analysis. Brain Imaging and Behavior 3: 154-66.

Király A, Szabó N, Tóth E, Csete G, Faragó P, Kocsis K, Must A, Vécsei L, Kincses ZT. 2016. Male brain ages faster: the age and gender dependence of subcortical volumes. Brain Imaging and Behavior 10: 901–10.

Kiselev VG, Hahn KR, Auer DP. 2003. Is the brain cortex a fractal? NeuroImage 20: 1765-74.

Lee JM, Yoon U, Kim JJ, Kim IY, Lee DS, Kwon JS, Kim SI. 2004. Analysis of the hemispheric asymmetry using fractal dimension of a skeletonized cerebral surface. IEEE Transactions on Biomedical Engineering 51: 1494-98.

Li S, Quan T, Xu C, Huang Q, Kang H, Chen Y, Li A, Fu L, Luo Q, Gong H, Zeng S. 2019. Optimization of traced neuron skeleton using Lasso-based model. Frontiers in Neuroanatomy 13:18.

Madan CR, Kensinger EA. 2016. Cortical complexity as a measure of age-related brain atrophy. NeuroImage 134: 617-29.

Mandelbrot BB. 1982. The fractal geometry of nature. San Francisco: W.H. Freeman and Company.

Maryenko NI, Stepanenko OY. 2022a. Fractal dimension of skeletonized MR images as a measure of cerebral hemispheres spatial complexity. Reports of Morphology 28: 40-47.

Maryenko NI, Stepanenko OY. 2022b. Shape of cerebral hemispheres: structural and spatial complexity. Quantitative analysis of skeletonized MR images. Reports of Morphology 28: 62-73.

Maryenko N, Stepanenko O. 2023. Quantitative characterization of age-related atrophic changes in cerebral hemispheres: A novel "contour smoothing" fractal analysis method. Translational Research in Anatomy 33: 100263.

Milosević NT, Ristanović D. 2006. Fractality of dendritic arborization of spinal cord neurons. Neurosci Lett 396: 172-76.

Podgórski P, Bladowska J, Sasiadek M, Zimny A. 2021. Novel volumetric and surface-based magnetic resonance indices of the aging brain - does male and female brain age in the same way? Frontiers in Neurology 12: 645729.

Savic I, Arver S. 2011. Sex dimorphism of the brain in male-to-female transsexuals. Cerebral Cortex (New York, N.Y.: 1991) 21: 2525–33.

Schneider CA, Rasband WS, Eliceiri KW. 2012. NIH Image to ImageJ: 25 years of image analysis. Nature Methods 9: 671-75.

Zhang L, Liu JZ, Dean D, Sahgal V, Yue GH. 2006. A three-dimensional fractal analysis method for quantifying white matter structure in human brain. Journal of neuroscience methods 150: 242-53.

Zhang L, Dean D, Liu JZ, Sahgal V, Wang X, Yue GH. 2007. Quantifying degeneration of white matter in normal aging using fractal dimension. Neurobiology of Aging 28: 1543-55.

Zhang L, Butler AJ, Sun CK, Sahgal V, Wittenberg GF, Yue GH. 2008. Fractal dimension assessment of brain white matter structural complexity post-stroke in relation to upper-extremity motor function. Brain Research 1228: 229-40.